Nanostructures

DOI: 10.1002/anie.201002024

Metal Nanocrystals with Highly Branched Morphologies

*Byungkwon Lim and Younan Xia**

aggregation · crystal growth · dendritic structures · nanoparticle synthesis · nanostructures

Metal nanocrystals with highly branched morphologies are an exciting new class of nanomaterials owing to their unique structures, physicochemical properties, and great potential as catalysts, sensing materials, and building blocks for nanoscale devices. Various strategies have recently been developed for the solution-phase synthesis of metal nanocrystals with branched morphologies, such as multipods and nanodendrites. In this Minireview, the procedures and mechanisms underlying the formation of branched metal nanocrystals are presented in parallel with recent advances in synthetic approaches based on kinetically controlled overgrowth, aggregation-based growth, heterogeneous seeded growth, selective etching, and template-directed methods, as well as their properties for catalytic or electrocatalytic applications.

1. Introduction

Controlling the morphology of a metal nanocrystal is critical to modern materials chemistry because its physical and chemical properties can be easily and widely tuned by tailoring the size and shape.[1] Combined with ease of synthesis and processing, metal nanocrystals with designed functions are promising candidates for a wide variety of applications in catalysis,[2] sensing,[3] imaging,[4] electronics,[5] photonics,[6] and medicine.[7] In most of these applications, shape control of metal nanocrystals is essential to not only maximize their performance but also fully exploit the potential of these remarkable nanoscale materials.

Among various possible morphologies that can be taken by a metal nanocrystal, multipods are of particular interest, both from an academic point of view and for the potential use as building blocks in the fabrication of complex nanoscale devices. Multipods formed from type II–VI semiconductors, such as CdSe, CdS, and CdTe, can be produced through crystal phase control by utilizing their polytypism; that is, the existence of different crystal structures in the same crystal. For example, a CdTe tetrapod consists of a zinc blende core (cubic crystal structure) and four wurtzite pods (hexagonal crystal structure).[8] However, nanocrystals formed from noble metals that crystallize only in a face-centered cubic (fcc) structure have no intrinsic driving force for growing into such highly anisotropic nanostructures, making the solution-phase synthesis of metal multipods extremely challenging. Nanodendrites formed from metals are another class of interesting nanostructures that are highly attractive for catalytic[9] or sensing-based applications.[10]

During the past decade, shape-controlled synthesis of colloidal metal nanocrystals in solution has advanced remarkably,[1,11] and it is now possible to generate highly branched nanostructures, such as multipod and nanodendrite, for various metals, including Pt,[9,12] Pd,[13] Au,[14] Ag,[10,15] and Rh.[16] Early syntheses of branched metal nanocrystals, however, have been largely achieved empirically, and the mechanisms responsible for anisotropic growth of multipods or nanodendrites were not discovered and understood until very recently. Rigorous understanding of growth mechanisms involved in the solution-phased synthesis of branched metal nanocrystals will enable us to design and generate more complex nanostructures with novel catalytic, optical, and electronic properties.

In this Minireview, we discuss how metal nanocrystals can grow into highly branched morphologies, in parallel with recent advances in synthetic approaches based on kinetically controlled overgrowth, aggregation-based growth, heterogeneous seeded growth, selective etching, and template-directed methods (Figure 1). We focus only on systems where there are already some reasonable understanding and experimental evidence for the growth mechanisms. Finally, we deal with a few examples to highlight the properties of branched metal nanocrystals for catalytic and electrocatalytic applications.

[*] Dr. B. Lim,[+] Prof. Y. Xia
Department of Biomedical Engineering, Washington University
St. Louis, MO 63130 (USA)
E-mail: xia@biomed.wustl.edu

[+] Current address: School of Advanced Materials Science and Engineering, Sungkyunkwan University, Suwon 44-746 (Korea)

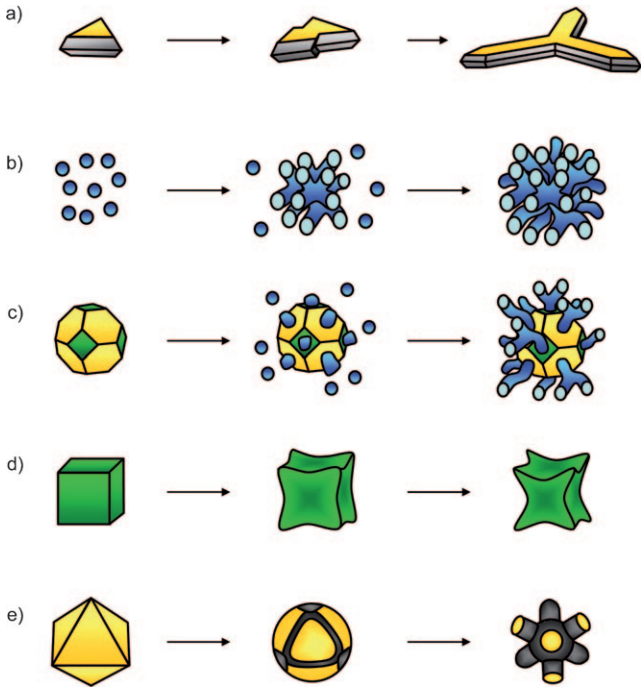

Figure 1. Various pathways that can lead to branched metal nanocrystals: a) anisotropic overgrowth into a multipod (modified with permission from Ref. [12h], copyright 2007 American Chemical Society); b) aggregation-based growth into a nanodendrite; c) aggregation-based growth in the presence of a foreign nanocrystal seed and formation of a bimetallic nanodendrite; d) selective etching on the faces and edges coupled with overgrowth along the corners (modified with permission from Ref. [12o], copyright 2009 American Chemical Society); and e) selective etching on the corners and edges (modified with permission from Ref. [15e], copyright 2010 American Chemical Society).

2. Multipods from Nanocrystal Overgrowth

In a solution-phase synthesis, nanocrystals of fcc metals tend to take a polyhedral shape, such as a truncated octahedron, cube, octahedron, icosahedron, and decahedron, depending on the twin structure of the seed and the ratios between growth rates of different crystallographic facets.[1,11] Compared to a polyhedral nanocrystal of the same volume, a nanocrystal in a highly branched morphology such as a multipod has a larger surface area and thus higher surface energy. As a result, formation of multipod-shaped nanocrystals is not favored in terms of thermodynamics and requires growth under kinetic control. At low growth rates, a nanocrystal may undergo a relaxation process during the course of growth in which adatoms can migrate on the nanocrystal surface to minimize the total surface energy,[17] and accordingly a polyhedral nanocrystal covered by low-index facets will be obtained. When the growth rate is increased beyond the thermodynamically controlled regime, anisotropic overgrowth can occur owing to a faster rate of atomic addition than that of adatom diffusion, with high-energy facets growing more quickly than low-energy facets.[18]

Various approaches have been developed to achieve anisotropic overgrowth of nanocrystal seeds into multipods. For example, we have demonstrated a kinetically controlled, polyol synthesis as an effective strategy for producing multipod-shaped platinum nanocrystals.[12c] In this approach, iron(III) species, coupled with O_2 existing in the polyol process, was employed as an etchant for platinum atoms to keep the initial concentration of platinum seeds at an extremely low level. By switching from air to a N_2 atmosphere, oxidative etching was blocked so that the concentration of platinum atoms abruptly increased to a high level. The generation of a high concentration of platinum atoms at a low concentration of platinum seeds accelerated the growth kinetics, leading to the overgrowth of the seeds into multipods that contained between two to six arms (Figure 2a).

Recently, Tilley and co-workers reported the synthesis of multipod-shaped palladium nanocrystals (Figure 2b) by room-temperature reduction of bis(acetonitrile) palladium(II) chloride under high-pressure H_2 in the presence of oleylamine and oleic acid as co-surfactants.[13c] They monitored the growth rate of palladium nanocrystals under different reaction conditions and stages using the in situ synchrotron X-ray diffraction technique, and confirmed the formation of palladium multipods at high growth rates. As expected, polyhedral nanocrystals with an icosahedral shape were obtained at low growth rates. They also observed the occurrence of secondary branching in random directions

Younan Xia was born in Jiangsu, China, in 1965. He studied at the University of Science and Technology of China (USTC), at the Fujian Institute of Research, and at the University of Pennsylvania (M.S. 1993, Alan G. MacDiarmid). He received a Ph.D. degree in physical chemistry from Harvard University (1996, George M. Whitesides). He started as an Assistant Professor of Chemistry at the University of Washington in Seattle in 1997, where he was made Associate Professor and Professor in 2002 and 2004, respectively. In 2007, he relocated to Washington University in St. Louis to take the position of James M. McKelvey Professor for Advanced Materials in the Department of Biomedical Engineering. His current research centers on the design and synthesis of nanostructured materials with controllable properties.

Byungkwon Lim was born in Seoul, Korea, in 1975. He studied at the School of Chemical and Biological Engineering at Seoul National University, Korea (B.S. 1998, M.S. 2000, Ph.D. 2004). He then worked on the synthesis and structural analysis of polymers for three years in the R&D Center of LG Chem, Korea. He has been working with Younan Xia as a post-doctoral fellow since 2007 and started as an Assistant Professor at Sungkyunkwan University in Korea in 2010. His research interests include the synthesis of nanostructured materials with controlled morphology, catalysis, self-assembly, and the fabrication of flexible devices.

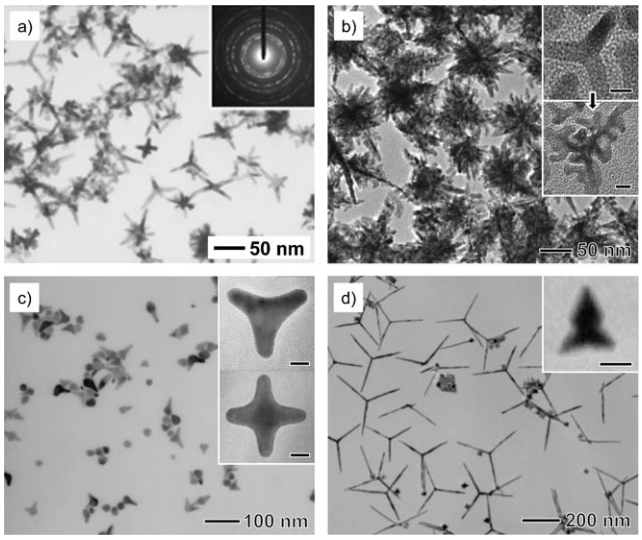

Figure 2. Various types of multipod-shaped metal nanocrystals: a) Pt multipods prepared by manipulating the growth kinetics of a polyol process (modified from Ref. [12c]); b) Pd multipods prepared by room-temperature reduction of bis(acetonitrile) palladium(II) chloride under 3 bar H_2 in the presence of oleylamine and oleic acid as co-surfactants (modified with permission from Ref. [13c], copyright 2010 American Chemical Society); c) Au multipods prepared by room-temperature reduction of $HAuCl_4$ in an aqueous solution with L-ascorbic acid as a reducing agent in the presence of CTAB, a trace amount of pre-formed Ag nanoplates, and NaOH (modified with permission from Ref. [14a], copyright 2003 American Chemical Society); and d) planar Pt tripods prepared by the reduction of $[Pt(acac)_2]$ in diphenyl ether with 1-adamantanecarboxylic acid and 1-hexadecylamine as capping agents (modified with permission from Ref. [12h], copyright 2007 American Chemical Society). All of the scale bars in the insets correspond to 10 nm.

during the growth of primary pods (Figure 2b, insets), which can be attributed to an enhanced growth rate at the later stages of the synthesis.

Multipods consisting of pods with high aspect ratios are rarely observed for gold. This might be related to a high diffusion coefficient for gold.[19] Lowering the reaction temperature may help decrease the tendency towards faceting and thus encourage anisotropic overgrowth. Chen and co-workers obtained a mixture of gold multipods with various morphologies (Figure 2c), such as monopod (25%), bipod (23%), tripod (9%), and tetrapod (3%), from room-temperature, aqueous-phase reduction of $HAuCl_4$ with L-ascorbic acid as a reducing agent in the presence of a high concentration of cetyltrimethylammonium bromide (CTAB) and a trace amount of pre-formed silver nanoplates.[14a] Sodium hydroxide was also used to accelerate the formation of gold multipods. Monopods and bipods were recognized as the intermediate products formed at different stages of pod growth towards tripod and tetrapod structures. It was suggested that the self-assembled structures of concentrated CTAB might play an important role in the formation of multipod shapes. In a related study, Schatz and co-workers observed that the reaction was substantially accelerated when both H_2O_2 and sodium citrate were employed as co-reductants for room-temperature reduction of $HAuCl_4$ in an aqueous solution, and gold tripods could be obtained in 40–50% yields.[14b] Gold multipods have also been prepared using a homogeneous seeded growth method.[14c] The synthesis was conducted at room temperature by reducing $HAuCl_4$ with L-ascorbic acid in the presence of CTAB and varying amounts of pre-formed gold seeds, and multipod-shaped gold nanocrystals were obtained (70% yield) only when a high concentration ratio of gold(III) ions to gold seeds was used to accelerate the growth kinetics.

In multipod formation, the twin structure of the seeds can also play an important role in controlling the number and/or symmetry of resultant pods. In an approach that is based on the reduction of a $[Pt(acac)_2]$ precursor in an organic medium, Yang and co-workers obtained planar platinum tripods in 25% yield (Figure 2d).[12h] A detailed electron microscopy study revealed that the tripods were formed by overgrowth along the three corners of a triangular seed containing a single {111} twin plane parallel to its top and bottom faces (Figure 2d, inset; see also Figure 1a). Other than the tripods, monopods and bipods were also obtained in the same synthesis, which were believed to grow from icosahedral or decahedral seeds with multiple twin defects. Schatz and co-workers also suggested the formation of their gold tripods by overgrowth of triangular seeds that were found in the same batch.[14b]

As can be seen in these examples, and especially for platinum and palladium, multipods formed by the overgrowth mechanism feature straight pods with high aspect ratios, which could be a unique signature for differentiating between them and other types of branched nanostructures formed by either aggregation or etching (see Sections 3–5). However, by far, most of the as-synthesized multipods were usually mixtures of those with varying dimension and number of pods and relatively low in terms of yield. A high level of architectural control of metal multipods prepared in the solution phase still remains a formidable challenge. To accomplish this goal, both the growth kinetics and the twin structures of the seeds should be more precisely controlled. The selection of an appropriate capping or stabilizing agent might also be one of the prerequisites for achieving a multipod morphology, although the effect of capping on pod growth is yet to be understood.

3. Dendritic Nanostructures from Aggregation-Based Nanocrystal Growth

Recent experimental studies have shown that particle coalescence or attachment can play an important role in nanocrystal growth.[17,20] Particle attachment is more commonly observed among small particles, because of both their higher energy owing to a larger surface-to-volume ratio and of a higher collision frequency associated with their greater mobility. In aggregation-based nanocrystal growth, the reduction in surface energy is achieved by eliminating pairs of surfaces, which provides a strong thermodynamic driving force for particle attachment.[20a,b]

If nanoparticles are allowed to diffuse by Brownian motion, they are likely to aggregate in a diffusion-controlled

manner, and accordingly dendritic growth can occur.[21] One of the first computational works supporting the dendritic growth by diffusion-limited aggregation (DLA) was reported by Witten and Sander in 1981,[22] who used a simple, square lattice model in which randomly diffusing particles are added, one at a time, to a growing aggregate of particles. They confirmed the generation of a large aggregate characterized by a randomly branching, open dendritic structure, as well as structural self-similarity (Figure 3). In the case of DLA model, the probability of finding a randomly diffusing particle around the core is extremely low owing to the so-called "screening effect" arising from the fact that the tips of most advanced branches capture the incoming, randomly diffusing particles most effectively.[21] It should be noted that a diffusion-limited aggregate arises only when the concentration of particles is low so that the aggregation process is governed by diffusion only.

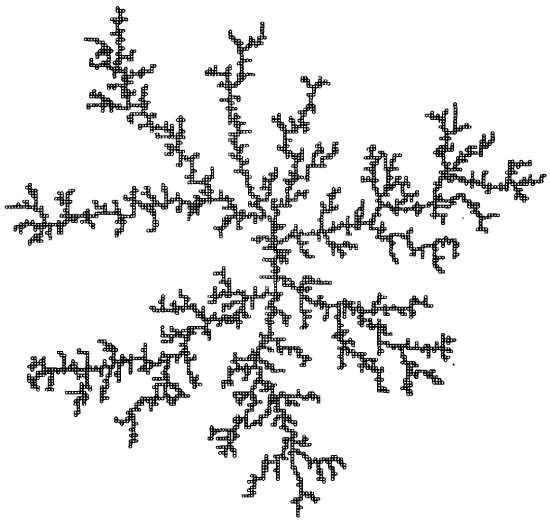

Figure 3. A diffusion-limited aggregate consisting of 3600 particles on a square lattice obtained by computer simulation (modified with permission from Ref. [22], copyright 1981 American Physical Society).

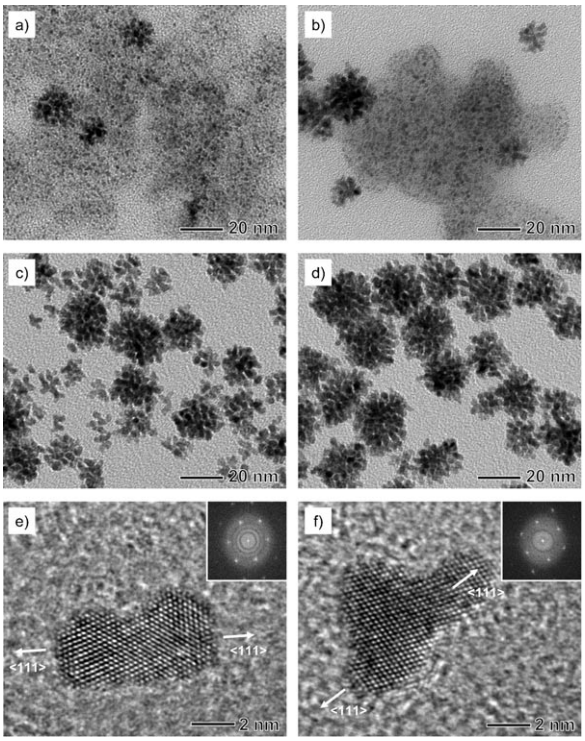

Figure 4. a–d) Transmission electron microscopy (TEM) images showing the morphological evolution of Pt nanodendrites. The reaction was conducted by reducing K_2PtCl_4 with L-ascorbic acid as a reducing agent in water and in the presence of PVP as a stabilizer. Reaction time: a) 1; b) 2; c) 5; and d) 10 min. e, f) High-resolution TEM (HRTEM) images of small Pt aggregates obtained at 5 min into the reaction (modified with permission from Ref. [24], copyright 2010 Springer).

Three-dimensional dendritic nanostructures have often been observed in the synthesis of platinum nanocrystals that involved the aqueous-phase reduction of a platinum salt precursor, such as K_2PtCl_4, by L-ascorbic acid in the presence of a polymeric stabilizer or surfactant, such as poly(vinyl pyrrolidone) (PVP), Pluronic F127 block polymer, tetradecyltrimethylammonium bromide, or sodium dodecyl sulfate.[12a,g,m,n] In most of these studies, a mechanism based on slow nucleation and fast growth mediated by autocatalytic reduction[23] has been proposed to explain the formation of dendritic nanostructures. Our recent study, however, has shown that this type of platinum nanostructures prepared with L-ascorbic acid is indeed a result of self-aggregation of initially formed, small platinum particles rather than overgrowth (Figure 4; see also Figure 1b).[24] As shown in Figure 4a, a large number of small platinum particles (less than 3 nm in diameter) emerged at the very early stages of the synthesis along with some large particles with varying degrees of aggregation. The number of small particles decreased with prolonged reaction times (Figure 4b,c), and they eventually disappeared completely, leaving behind platinum nanodendrites (Figure 4d), indicating that growth proceeded by particle attachment. Small platinum aggregates composed of a few particles exhibited an either linear or branched structures (Figure 4e,f). Their lattice fringes are perfectly aligned along the long axis, indicating that they were formed by the oriented attachment mechanism.[20] In the oriented attachment process, adjacent particles self-organize so that they share a common crystallographic orientation. However, it was shown that the Pt nanodendrites have a polycrystalline nature,[12n,24] which can be attributed to the involvement of twinning and/or imperfect oriented attachment characterized by a small misorientation at the interface.[25] Nanodendrites with dense cores probably arise from the generation of a high concentration of particles at the very early stages of the synthesis, wherein particles may not follow the aggregation process predicted by a simple DLA model. Formation of dense cores by extensive self-aggregation could be avoided to some extent by decreasing the concentration of a platinum precursor involved in the synthesis.[12m] Similar dendritic (or foam-like) morphologies have also been observed for other metals, such as Ni, Ru, and Rh, and their growth mechanism was attributed to the DLA.[26]

4. Bimetallic Nanodendrites by Heterogeneous Seeded Growth

Heterogeneous seeded growth has recently emerged as a powerful tool for precisely controlling the morphology and composition of bimetallic nanocrystals[27] in which pre-formed nanocrystals serve as seeds for further growth of another metal with a different chemical identity. This approach has also enabled the preparation of bimetallic nanocrystals with highly branched morphologies, such as nanodendrites consisting of branched arms formed from one metal supported on the core of another metal. For example, Au-Pt bimetallic nanodendrites have been synthesized by the reduction of $[Pt(acac)_2]$ in an organic medium such as an oleylamine/diphenyl ether or oleylamine/decahydronaphthalene mixture in the presence of gold nanocrystals as seeds.[28]

Recently, we reported a simple, aqueous route to the synthesis of bimetallic nanodendrites consisting of a dense array of platinum branches on a palladium nanocrystal core (Figure 5).[29] In this new approach, truncated octahedral nanocrystals of palladium with an average size of 9 nm were used as seeds to direct the dendritic growth of platinum upon the reduction of K_2PtCl_4 by L-ascorbic acid in an aqueous solution. The resultant Pd-Pt nanodendrites exhibited a three-dimensional dendritic morphology, with platinum branches being distributed over the entire surface of the palladium seed. Another interesting feature of this unique nanostructure is an epitaxial relationship between the palladium core and the platinum branches (Figure 5d), which can be attributed to the close lattice match between these two metals (Pd and Pt have a lattice mismatch of only 0.77%). A similar structure was also observed by Peng and Yang for Pd-Pt bimetallic nanocrystals, in which $[Pt(acac)_2]$ was reduced in an oleylamine/diphenyl ether mixture containing palladium nanocrystals as seeds.[30]

In our most recent study, it was found that both homogeneous and heterogeneous nucleation of platinum occurred at the very early stages of the synthesis of the Pd-Pt nanodendrites and the growth of platinum branches proceeded by attachment of small platinum particles that had been formed by homogenous nucleation in the solution (Figure 6; see also Figure 1c).[24] These observations contradict the previously suggested mechanisms that only consider heterogeneous nucleation and subsequent growth by atomic addition[28,29] and suggest that homogeneous nucleation and particle attachment might also play important roles in heterogeneous seeded growth of other types of bimetallic nanodendrites. It is also worth pointing out that unlike the pure platinum nanodendrites discussed in Section 3, the Pd-Pt nanodendrites exhibited a more open dendritic structure without significant overlap between platinum branches despite the fact that both nanostructures not only originated from the same growth mechanism based on particle attachment but also were prepared at the same concentration of the platinum precursor.[24,29] The truncated octahedral palladium seeds seem to play a pivotal role in initiating and maintaining an

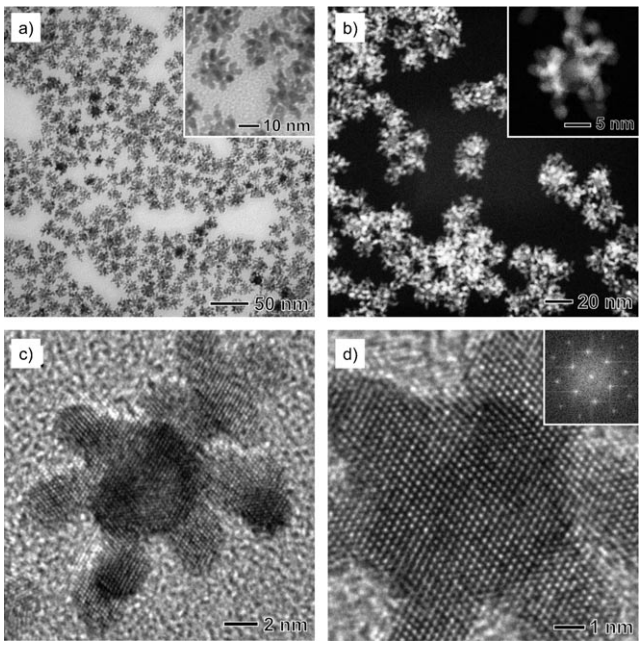

Figure 5. Electron microscopy characterization of Pd-Pt bimetallic nanodendrites synthesized by reducing K_2PtCl_4 with L-ascorbic acid as a reducing agent in the presence of truncated octahedral Pd seeds in an aqueous solution: a) TEM; b) high-angle annular dark-field scanning TEM; and c,d) HRTEM images (modified with permission from Ref. [29], copyright 2009 American Association for the Advancement of Science).

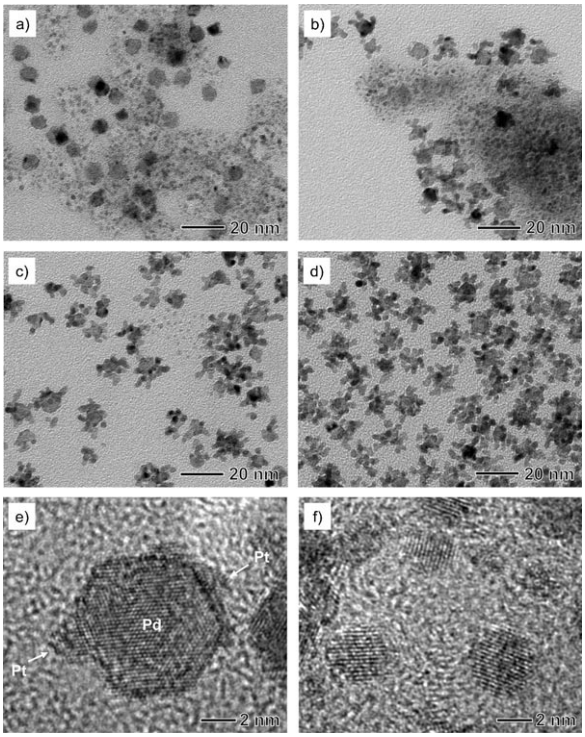

Figure 6. a–d) TEM images showing the morphological evolution of the Pd-Pt nanodendrites shown in Figure 5. Reaction time: a) 1; b) 2; c) 5; and d) 10 min. e, f) HRTEM images taken from the sample shown in (a): e) a Pd-Pt particle containing Pt bumps formed by heterogeneous nucleation and f) small Pt particles formed by homogeneous nucleation in the solution (modified with permission from Ref. [24], copyright 2010 Springer).

open dendritic structure by providing multiple sites for particle attachment that are spatially separated from each other, making it possible to avoid overlap and fusion between the growing platinum branches. This synthetic strategy based on heterogeneous seeded growth could be extended to produce dendritic metal nanostructures with a number of branching generations and/or variations in the composition whilst maintaining a highly open structure.

5. Branching via Selective Etching

Corrosion is a familiar and common phenomenon in nature, and may take place in many different forms, such as etching, pitting, galvanic replacement, and dealloying.[31] Although corrosion is generally undesirable, it can be exploited as a versatile route to metal nanostructures with unconventional morphologies. As mentioned in Section 2, if a nanocrystal synthesis is conducted in air in the presence of ligands such as halide ions or iron(III) species, oxidative etching can occur during the synthesis.[1] In previous studies on the shape-controlled synthesis of metal nanocrystals, etching has been utilized to control the crystallinity of seeds,[32] generate hollow structures,[33] and truncate sharp corners.[34] Recently, etching has also proven to be an extremely powerful method for transforming polyhedral metal nanocrystals into highly branched structures.

In a recent study, Tilley and co-workers observed the successive transformation of nanocubes into octapod-like structures and then highly branched structures during the synthesis of platinum nanocrystals that involved $[Pt(acac)_2]$ as a platinum precursor and a mixture of toluene and oleylamine as the medium (Figure 7).[12o] This morphological transformation was brought about by selective etching on the faces and edges of the nanocubes combined with an overgrowth process that occurred simultaneously and at comparable rates (see Figure 1d). Interestingly, etching was observed only in the reaction conducted at a high concentration of $[Pt(acac)_2]$. As no halide ions or O_2 was present in the reaction system, the authors suggested that the etchant originated from the acetylacetonate precursor or a by-product of acetylacetonate. Referring to the previous studies by Masel and co-workers,[35] the authors further suggested that an enol form of acetylacetone might serve as the etchant through a chelation process.

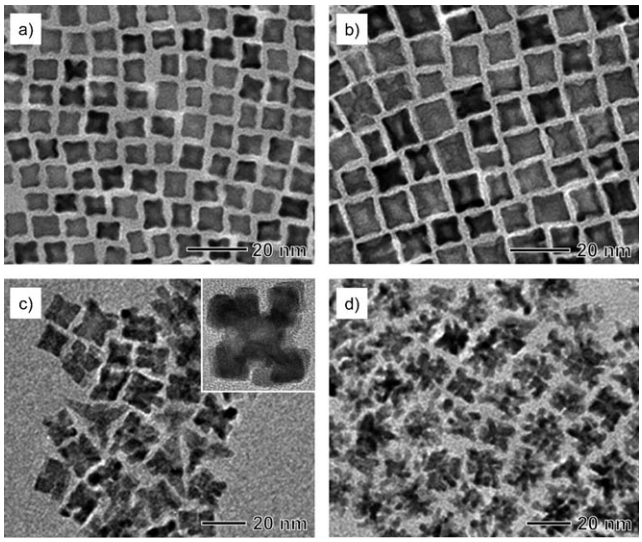

Figure 7. TEM images showing the morphological transformation of Pt nanocubes into branched structures by selective etching on the faces and edges of the nanocubes coupled with an overgrowth process. The reaction was conducted at a high concentration of $[Pt(acac)_2]$ in a mixture of toluene and oleylamine. Reaction time: a) 75; b) 120; c) 240; and d) 500 min (modified with permission from Ref. [12o], copyright 2009 American Chemical Society).

An interesting approach for multipod-shaped silver nanocrystals was recently reported by Yang and co-workers, who added an appropriate wet etchant to a suspension of the as-prepared octahedral silver nanocrystals.[15e] When exposed to an $NH_4OH/H_2O_2/CrO_3$ mixture with a relatively strong etching power, the silver octahedrons transformed into cubes with slightly rough surfaces, indicating that the corners of the octahedron were etched to the {100} faces of a cube. The use of an NH_4OH/H_2O_2 mixture as a relatively weak etchant made it possible to selectively etch the corners and edges of the octahedrons, resulting in the formation of octapod-shaped nanocrystals with the same symmetry of the starting octahedrons (Figure 8; see also Figure 1e). As the authors mentioned, the key to obtaining nanocrystals with a desired morphology was to choose an etchant with an appropriate strength: an etchant that is too strong may lead to isotropic etching, whereas an etchant that is too weak may not be able to react with the surface of a nanocrystal in the presence of capping agents.

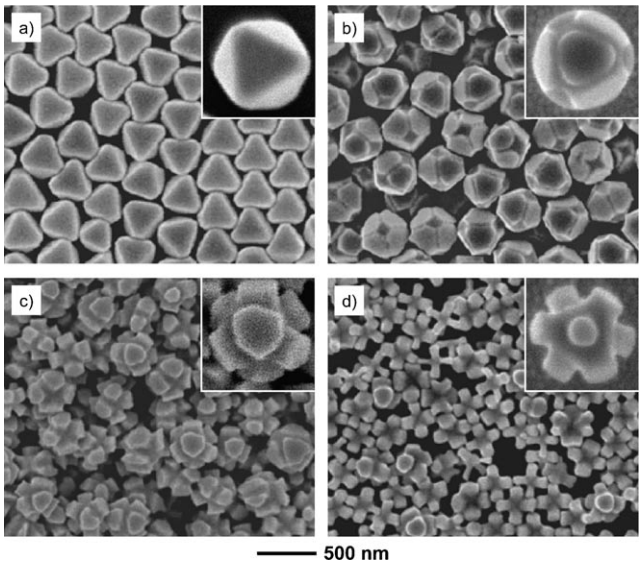

Figure 8. SEM images showing the etching progress of octahedral Ag nanocrystals: a) Ag octahedrons used as the starting material, and b–d) Ag nanocrystals obtained by exposing the octahedrons to increasing concentrations of NH_4OH/H_2O_2 etchant (modified with permission from Ref. [15e], copyright 2010 American Chemical Society).

6. Branched Nanocrystals from Template-Directed Synthesis

Template-directed synthesis has been widely used to generate inorganic nanostructures in high yields.[36] In general, the template serves as a scaffold, within (or around) which a different material is added (or produced in situ) and shaped into a nanostructure with its shape or morphology complementary to that of the template. Recently, we presented a template-directed method for generating gold multipods (Figure 9a).[14f] In this approach, a three-dimensionally porous lattice consisting of uniform iron nanoparticles that were self-assembled on a magnetic stirrer bar served as a template (Figure 9b). This unique template not only participated in the chemical reaction but also spontaneously fell apart at a certain point to release the products. Upon addition of AuCl, a galvanic replacement reaction took place between iron and gold(I), leading to the formation of highly branched gold nanostructures in the void space of the template (Figure 9c). During the reaction, both the volume expansion associated with Au/Fe replacement and the consumption of iron gradually weakened the attraction between the iron nanoparticles, and eventually the lattice of iron nanoparticles spontaneously fell apart to automatically release the gold multipods (Figure 9d). The remaining iron nanoparticles could be readily removed by washing the samples with an acid such as H_2SO_4 or HNO_3 to dissolve the unreacted iron. The as-obtained gold multipods were mainly composed of branched arms as shown in Figure 9e. Compared to the traditional template-directed methods, this approach is characterized by a number of distinctive features: 1) the system works on a scale almost 100 times smaller than those based on latex spheres to produce inverse opals; 2) the template itself is also directly involved in the reaction; 3) the template spontaneously disassembles during the synthesis; and 4) the final product has a highly branched morphology. This strategy can potentially be extended to other metal systems.

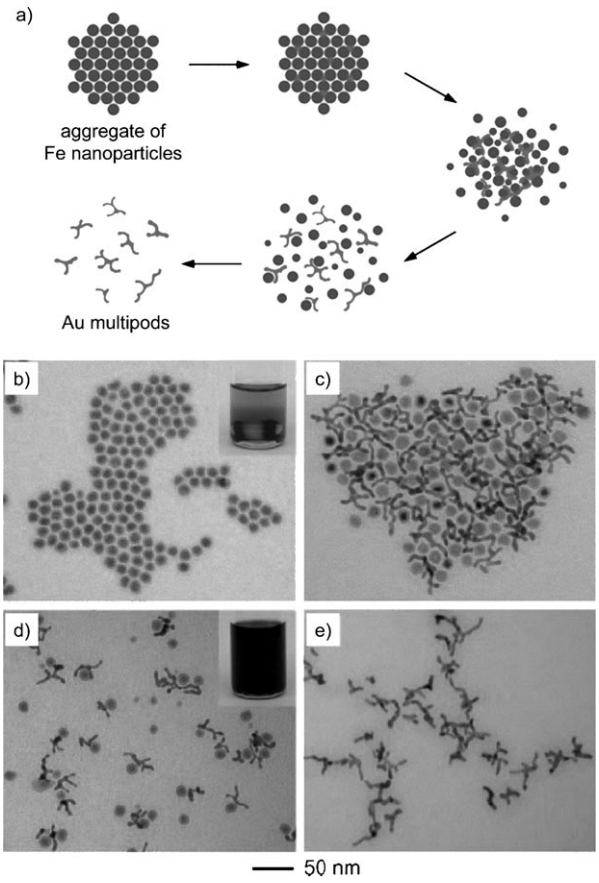

Figure 9. a) Formation of Au multipods by templating against a self-destructive lattice of Fe nanoparticles: 1) Au nucleates in the voids of aggregated Fe nanoparticles through a replacement reaction between Fe and Au^{I}; 2) Au evolves into multipods; and 3) Au multipods are harvested and purified by dissolving the remaining Fe nanoparticles with H_2SO_4. TEM images of b) Fe nanoparticles, c) the sample obtained after adding a Au precursor, d) completely disassembled Fe nanoparticles and Au multipods, and e) Au multipods after removing the remaining Fe (modified from Ref. [14f]).

7. Catalytic Properties and Applications

Catalysis has long relied on noble metal nanocrystals for a wide variety of chemical and electrochemical reactions.[2] Noble metal nanocrystals with highly branched structures are of particular interest for catalysis, as they generally exhibit a reasonably large specific surface area and a high specific activity (that is, activity per unit surface area) owing to high densities of edges, corners, and stepped atoms present on their branches. In a number of studies, branched metal nanocrystals have shown great promise for use as catalysts or electrocatalysts with substantially enhanced activity.[12i,j,14e,24,28–30] For instance, El-Sayed and co-workers investigated the catalytic properties of multi-armed platinum nanocrystals prepared using tetrahedral platinum nanocrystals as seeds for the electron-transfer reaction between hexacyanoferrate(III) and thiosulfate.[12i] These multi-armed platinum nanocrystals could lower the activation energy of the reaction by 1.6 times as compared to the tetrahedral nanocrystals thanks to the presence of more edges and corners as well as high-index facets on the arms. Sun and co-workers have recently shown that star-shaped gold nanocrystals, prepared by the reduction of $HAuCl_4$ with L-ascorbic acid in a deep eutectic solvent, exhibited a much higher specific activity towards the electrocatalytic reduction of H_2O_2 than a polycrystalline gold electrode. This higher activity was attributed to the high density of stepped atoms on the surface.[14e]

Proton-exchange membrane (PEM) fuel cells hold great potential for a variety of applications, including powering transportation vehicles, portable electronic devices, and on-site power generation.[37] However, the sluggish kinetics of the oxygen reduction reaction (ORR) at the cathode of a PEM fuel cell has been identified as one of the main limitations for commercialization.[38] In recent studies, we applied the Pd-Pt bimetallic nanodendrites (discussed in Section 4) as a novel class of electrocatalysts for PEM fuel cell applications.[24,29] In an initial study,[29] it was found that the Pd-Pt nanodendrites had a specific electrochemically active surface area (ECSA) of 57.1 $m^2 g_{Pt}^{-1}$ on the basis of the platinum mass, which was 77% of the commercial Pt/C catalyst (74.0 $m^2 g_{Pt}^{-1}$) and three

times that of the commercial platinum-black catalyst (19.1 $m^2 g_{Pt}^{-1}$), demonstrating that the highly branched structure of the Pd-Pt nanodendrites provided a reasonably high surface area despite their relatively large overall particle size. At room temperature and 0.9 V versus a reversible hydrogen electrode (RHE), the Pd-Pt nanodendrites were two and a half times more active on the basis of equivalent platinum mass for the ORR than the Pt/C catalyst and five times more active than the platinum-black catalyst (Figure 10a,b). In addition to the mass activity, the Pd-Pt nanodendrites also exhibited a specific activity of 3.1 to 3.4 times that of the Pt/C catalyst and 1.7 to 2.0 times that of the platinum-black catalyst depending on the temperature, indicating the accelerated ORR kinetics on the surfaces of the Pd-Pt nanodendrites. The higher ORR activity of the Pd-Pt nanodendrites was attributed to the reasonably high surface area intrinsic to the dendritic morphology and the preferential exposure of particularly active facets, such as {111}, {110}, and {311}, towards ORR on the palladium-supported platinum branches. In a subsequent study,[24] the specific ECSA of the Pd-Pt nanodendrites was found to be almost twice that of the pure platinum nanodendrites (28.8 $m^2 g_{Pt}^{-1}$), discussed in Section 3, demonstrating that the open dendritic structure enabled a higher surface area. It was also found that the Pd-Pt nanodendrites were up to three times more active on the basis of equivalent platinum mass for the ORR and up to two times more active for the oxidation of formic acid (Figure 10c,d) as compared to the platinum nanodendrites. These results suggest that a synthetic methodology based on heterogeneous seeded growth provides a more efficient way for generating platinum-based electrocatalysts with improved activities. Very recently, Wang and co-workers successfully prepared Pd-Pt bimetallic nanodendrites supported on graphene nanosheets by growing platinum branches directly on the graphene-supported palladium nanocrystal seeds, with their mass activity for the methanol oxidation reaction being about 3.0 and 9.5 times greater than that of the commercial Pt/C and platinum-black catalysts, respectively.[39]

From the results discussed in this section, it is clear that metal nanocrystals with highly branched morphologies hold great potential for both catalytic or electrocatalytic applications. However, several issues regarding catalyst stability and large-scale production still need to be addressed before such branched metal nanocrystals can be commercialized as industrial catalysts.

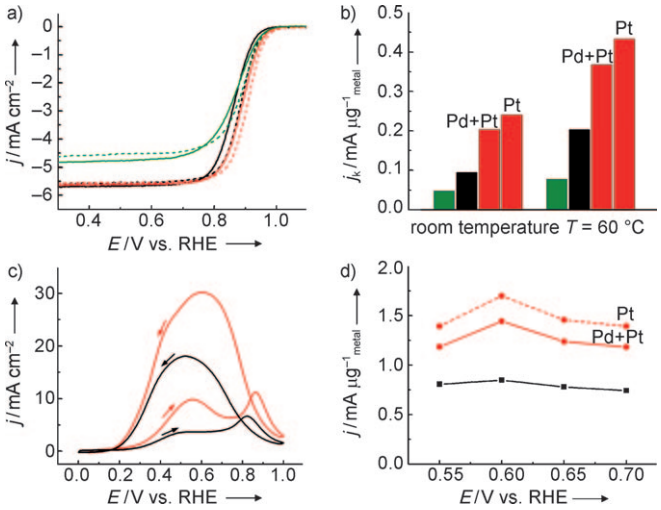

Figure 10. a,b) Comparison of electrocatalytic properties of the Pd/Pt nanodendrites (shown in Figure 5; red lines and bars), Pt/C catalyst (E-TEK, 20% by weight of 3.2 nm Pt nanoparticles on carbon support; black lines and bars), and Pt black (Aldrich, fuel-cell grade; green lines and bars) for the ORR: a) ORR polarization curves recorded at room temperature (solid lines) and 60 °C (dashed lines) in O_2-saturated 0.1 M $HClO_4$ solutions and b) mass activities at 0.9 V versus RHE (modified with permission from Ref. [29], copyright 2009 American Association for the Advancement of Science). c,d) Comparison of electrocatalytic properties of the Pd/Pt nanodendrites (red lines) and the Pt nanodendrites (black lines), shown in Figure 4d, for the formic acid oxidation reaction: c) CV curves recorded at room temperature in 0.25 M HCOOH + 0.5 M H_2SO_4 solutions and d) mass activities (modified with permission from Ref. [24], copyright 2010 Springer). For the Pd/Pt nanodendrites, Pt nanodendrites, and Pt/C catalyst, the metal loading on a glassy carbon electrode was 15.3 μg cm^{-2}, whereas the metal loading was 40.8 μg cm^{-2} for the Pt-black catalyst. In (b) and (d), both the Pt mass and (Pd + Pt) mass activities are shown for the Pd/Pt nanodendrites.

8. Summary and Outlook

Recent years have witnessed rapid and significant progress in the shape-controlled synthesis of metal nanocrystals. However, the controlled synthesis and the applications of branched metal nanocrystals are still at the infancy stage compared to those of nanocrystals with conventional shapes such as polyhedrons. The synthesis of branched metal nanocrystals is of great importance not only from an academic point of view but also for the development of next-generation catalysts with substantially enhanced performance for a wide variety of chemical and electrochemical reactions. It is reasonable to expect that branched metal nanocrystals may also find use in many applications beyond catalysis, such as sensing, imaging, and nanoscale fabrication.

In this Minireview, we divided the strategies for the synthesis of branched metal nanocrystals into five categories: 1) kinetically controlled overgrowth; 2) aggregation-based growth; 3) heterogeneous seeded growth; 4) selective etching; and 5) the template-directed method. These methods could serve as the common strategies for preparation of branched metal nanocrystals. When these strategies were discussed, we only focused on a limited number of examples recently reported in the literature. It is worth noting that most of these strategies could be modified and further extended to different metal systems.

Deeper insights into growth mechanisms for branched metal nanocrystals will help determine the optimal conditions necessary to obtain the product in a controllable and reproducible manner and design more complex metal nanostructures. There is no doubt that the field of synthesis and application of branched metal nanocrystals will keep moving forward as better understanding of their growth mechanisms and properties are achieved.

This work was supported in part by a research grant from NSF (DMR-0804088) and startup funds from Washington University in St. Louis.

Received: April 6, 2010
Published online: November 18, 2010

[1] Y. Xia, Y. Xiong, B. Lim, S. E. Skrabalak, *Angew. Chem.* **2009**, *121*, 62; *Angew. Chem. Int. Ed.* **2009**, *48*, 60.

[2] a) L. N. Lewis, *Chem. Rev.* **1993**, *93*, 2693; b) G. A. Somorjai, *Chem. Rev.* **1996**, *96*, 1223; c) G. Ertl, *Handbook of Heterogeneous Catalysis*, Wiley-VCH, Weinheim, **2008**.

[3] a) T. A. Taton, C. A. Mirkin, R. L. Letsinger, *Science* **2000**, *289*, 1757; b) A. G. Tkachenko, H. Xie, D. Coleman, W. Glomm, J. Ryan, M. F. Anderson, S. Franzen, D. L. Feldheim, *J. Am. Chem. Soc.* **2003**, *125*, 4700; c) X. Zhang, M. A. Young, O. Lyandres, R. P. Van Duyne, *J. Am. Chem. Soc.* **2005**, *127*, 4484; d) M. M.-C. Cheng, G. Cuda, Y. L. Bunimovich, M. Gaspari, J. R. Heath, H. D. Hill, C. A. Mirkin, A. J. Nijdam, R. Terracciano, T. Thundat, M. Ferrari, *Curr. Opin. Chem. Biol.* **2006**, *10*, 11; e) H. Wang, D. W. Brandl, P. Nordlander, N. J. Halas, *Acc. Chem. Res.* **2007**, *40*, 53.

[4] a) J. Chen, F. Saeki, B. J. Wiley, H. Cang, M. J. Cobb, Z.-Y. Li, L. Au, H. Zhang, M. B. Kimmey, X. Li, Y. Xia, *Nano Lett.* **2005**, *5*, 473; b) H. Cang, T. Sun, Z.-Y. Li, J. Chen, B. J. Wiley, Y. Xia, X. Li, *Opt. Lett.* **2005**, *30*, 3048; c) X. Yang, S. E. Skrabalak, Z.-Y. Li, Y. Xia, L. V. Wang, *Nano Lett.* **2007**, *7*, 3798.

[5] a) N. M. Davey, R. J. Seymour, *Platinum Met. Rev.* **1985**, *29*, 2; b) S. Jeong, K. Woo, D. Kim, S. Lim, J. S. Kim, H. Shin, Y. Xia, J. Moon, *Adv. Funct. Mater.* **2008**, *18*, 679.

[6] a) S. A. Maier, M. L. Brongersma, P. G. Kik, S. Meltzer, A. A. G. Requicha, H. A. Atwater, *Adv. Mater.* **2001**, *13*, 1501; b) A. W. Sanders, D. A. Routenberg, B. J. Wiley, Y. Xia, E. R. Dufresne, M. A. Reed, *Nano Lett.* **2006**, *6*, 1822.

[7] a) J. L. West, N. J. Halas, *Annu. Rev. Biomed. Eng.* **2003**, *5*, 285; b) P. K. Jain, I. H. El-Sayed, M. A. El-Sayed, *Nano Today* **2007**, *2*, 18; c) S. E. Skrabalak, J. Chen, L. Au, X. Lu, X. Li, Y. Xia, *Adv. Mater.* **2007**, *19*, 3177; d) S. E. Skrabalak, L. Au, X. Lu, X. Li, Y. Xia, *Nanomedicine* **2007**, *2*, 657; e) P. Fortina, L. J. Kricka, D. J. Graves, J. Park, T. Hyslop, F. Tam, N. Halas, S. Surrey, S. A. Waldman, *Trends Biotechnol.* **2007**, *25*, 145; f) L. Au, D. Zheng, F. Zhou, Z.-Y. Li, X. Li, Y. Xia, *ACS Nano* **2008**, *2*, 1645.

[8] a) L. Manna, E. C. Scher, A. P. Alivisatos, *J. Am. Chem. Soc.* **2000**, *122*, 12700; b) L. Manna, D. J. Milliron, A. Meisel, E. C. Scher, A. P. Alivisatos, *Nat. Mater.* **2003**, *2*, 382; c) D. J. Milliron, S. M. Hughes, Y. Cui, L. Manna, J. Li, L.-W. Wang, A. P. Alivisatos, *Nature* **2004**, *430*, 190.

[9] X. Teng, X. Liang, S. Maksimuk, H. Yang, *Small* **2006**, *2*, 249.

[10] Y. Wang, P. H. C. Camargo, S. E. Skrabalak, H. Gu, Y. Xia, *Langmuir* **2008**, *24*, 12042.

[11] a) Y. Sun, Y. Xia, *Science* **2002**, *298*, 2176; b) B. Wiley, Y. Sun, Y. Xia, *Acc. Chem. Res.* **2007**, *40*, 1067; c) Y. Xiong, Y. Xia, *Adv. Mater.* **2007**, *19*, 3385; d) A. R. Tao, S. Habas, P. Yang, *Small* **2008**, *4*, 310; e) B. Lim, M. Jiang, J. Tao, P. H. C. Camargo, Y. Zhu, Y. Xia, *Adv. Funct. Mater.* **2009**, *19*, 189; f) J. Chen, B. Lim, E. P. Lee, Y. Xia, *Nano Today* **2009**, *4*, 81.

[12] a) Y. Song, Y. Yang, C. J. Medforth, E. Pereira, A. K. Singh, H. Xu, Y. Jiang, C. J. Brinker, F. Swol, J. A. Shelnutt, *J. Am. Chem. Soc.* **2004**, *126*, 635; b) T. Herricks, J. Chen, Y. Xia, *Nano Lett.* **2004**, *4*, 2367; c) J. Chen, T. Herricks, Y. Xia, *Angew. Chem.* **2005**, *117*, 2645; *Angew. Chem. Int. Ed.* **2005**, *44*, 2589; d) X. Teng, H. Yang, *Nano Lett.* **2005**, *5*, 885; e) S. Maksimuk, X. Teng, H. Yang, *Phys. Chem. Chem. Phys.* **2006**, *8*, 4660; f) Y. Song, W. A. Steen, D. Pena, Y.-B. Jiang, C. J. Medforth, Q. Huo, J. L. Pincus, Y. Qiu, D. Y. Sasaki, J. E. Miller, J. A. Shelnutt, *Chem. Mater.* **2006**, *18*, 2335; g) H. Lee, S. E. Habas, S. Kweskin, D. Butcher, G. A. Somorjai, P. Yang, *Angew. Chem.* **2006**, *118*, 7988; *Angew. Chem. Int. Ed.* **2006**, *45*, 7824; h) S. Maksimuk, X. Teng, H. Yang, *J. Phys. Chem. C* **2007**, *111*, 14312; i) M. A. Mahmoud, C. E. Tabor, M. A. El-Sayed, Y. Ding, Z. L. Wang, *J. Am. Chem. Soc.* **2008**, *130*, 4590; j) B. Lim, X. Lu, M. Jiang, P. H. C. Camargo, E. C. Cho, E. P. Lee, Y. Xia, *Nano Lett.* **2008**, *8*, 4043; k) M. Tsuji, P. Jiang, S. Hikino, S. Lim, R. Yano, Sa.-M. Jang, S.-H. Yoon, N. Ishigami, X. Tang, K. S. N. Kamarudin, *Colloids Surf. A* **2008**, *317*, 23; l) L. Wang, S. Guo, J. Zhai, S. Dong, *J. Phys. Chem. C* **2008**, *112*, 13372; m) L. Wang, Y. Yamauchi, *Chem. Mater.* **2009**, *21*, 3562; n) L. Wang, Y. Yamauchi, *J. Am. Chem. Soc.* **2009**, *131*, 9152; o) S. Cheong, J. Watt, B. Ingham, M. F. Toney, R. D. Tilley, *J. Am. Chem. Soc.* **2009**, *131*, 14590.

[13] a) Y.-H. Chen, H.-H. Hung, M. H. Huang, *J. Am. Chem. Soc.* **2009**, *131*, 9114; b) J. Watt, N. Young, S. Haigh, A. Kirkland, R. D. Tilley, *Adv. Mater.* **2009**, *21*, 2288; c) J. Watt, S. Cheong, M. F. Toney, B. Ingham, J. Cookson, P. T. Bishop, R. D. Tilley, *ACS Nano* **2010**, *4*, 396.

[14] a) S. Chen, Z. L. Wang, J. Ballato, S. H. Foulger, D. L. Carroll, *J. Am. Chem. Soc.* **2003**, *125*, 16186; b) E. Hao, R. C. Bailey, G. C. Schatz, J. T. Hupp, S. Li, *Nano Lett.* **2004**, *4*, 327; c) T. K. Sau, C. J. Murphy, *J. Am. Chem. Soc.* **2004**, *126*, 8648; d) C. L. Nehl, H. Liao, J. H. Hafner, *Nano Lett.* **2006**, *6*, 683; e) H.-G. Liao, Y.-X. Jiang, Z.-Y. Zhou, S.-P. Chen, S.-G. Sun, *Angew. Chem.* **2008**, *120*, 9240; *Angew. Chem. Int. Ed.* **2008**, *47*, 9100; f) Z. Li, W. Li, P. H. C. Camargo, Y. Xia, *Angew. Chem.* **2008**, *120*, 9799; *Angew. Chem. Int. Ed.* **2008**, *47*, 9653; g) C. G. Khoury, T. Vo-Dinh, *J. Phys. Chem. C* **2008**, *112*, 18849.

[15] a) X. Wang, H. Itoh, K. Naka, Y. Chujo, *Langmuir* **2003**, *19*, 6242; b) X. Wen, Y.-T. Xie, M. W. C. Mak, K. Y. Cheung, X.-Y. Li, R. Renneberg, S. Yang, *Langmuir* **2006**, *22*, 4836; c) J. Fang, H. You, P. Kong, Y. Yi, X. Song, B. Ding, *Cryst. Growth Des.* **2007**, *7*, 864; d) X. Liu, R. Huang, J. Zhu, *Chem. Mater.* **2008**, *20*, 192; e) M. J. Mulvihill, X. Y. Ling, J. Henzie, P. Yang, *J. Am. Chem. Soc.* **2010**, *132*, 268.

[16] a) J. D. Hoefelmeyer, K. Niesz, G. A. Somorjai, T. D. Tilley, *Nano Lett.* **2005**, *5*, 435; b) N. Zettsu, J. M. McLellan, B. Wiley, Y. Yin, Z.-Y. Li, Y. Xia, *Angew. Chem.* **2006**, *118*, 1310; *Angew. Chem. Int. Ed.* **2006**, *45*, 1288; c) S. M. Humphrey, M. E. Grass, S. E. Habas, K. Niesz, G. A. Somorjai, T. D. Tilley, *Nano Lett.* **2007**, *7*, 785.

[17] a) H. Zheng, R. K. Smith, Y.-W. Jun, C. Kisielowski, U. Dahmen, A. P. Alivisatos, *Science* **2009**, *324*, 1309; b) B. Lim, H. Kobayashi, P. H. C. Camargo, L. F. Allard, J. Liu, Y. Xia, *Nano Res.* **2010**, *3*, 180.

[18] Y. Yin, A. P. Alivisatos, *Nature* **2005**, *437*, 664.

[19] a) P. Buffat, J.-P. Borel, *Phys. Rev. A* **1976**, *13*, 2287; b) R. Li, K. Sieradzki, *Phys. Rev. Lett.* **1992**, *68*, 1168; c) J. Erlebacher, M. J. Aziz, A. Karma, N. Dimitrov, K. Sieradzki, *Nature* **2001**, *410*, 450.

[20] a) J. F. Banfield, S. A. Welch, H. Zhang, T. T. Ebert, R. L. Penn, *Science* **2000**, *289*, 751; b) A. P. Alivisatos, *Science* **2000**, *289*, 736; c) C. Pacholski, A. Kornowski, H. Weller, *Angew. Chem.* **2002**, *114*, 1234; *Angew. Chem. Int. Ed.* **2002**, *41*, 1188; d) F. Huang, H. Zhang, J. F. Banfield, *J. Phys. Chem. B* **2003**, *107*, 10470; e) J. H. Yu, J. Joo, H. M. Park, S. I. Baik, Y. W. Kim, S. C. Kim, T. Hyeon, *J. Am. Chem. Soc.* **2005**, *127*, 5662; f) M. Niederberger, H. Cölfen, *Phys. Chem. Chem. Phys.* **2006**, *8*, 3271; g) A. Halder, N. Ravishankar, *Adv. Mater.* **2007**, *19*, 1854.

[21] T. Vicsek, *Fractal Growth Phenomena*, 2nd ed., World Scientific, Singapore, **1992**.

[22] T. A. Witten, L. M. Sander, *Phys. Rev. Lett.* **1981**, *47*, 1400.

[23] a) L. Colombi Ciacchi, W. Pompe, A. De Vita, *J. Am. Chem. Soc.* **2001**, *123*, 7371; b) L. Colombi Ciacchi, W. Pompe, A. D. Vita, *J. Phys. Chem. B* **2003**, *107*, 1755.

[24] B. Lim, M. Jiang, T. Yu, P. H. C. Camargo, Y. Xia, *Nano Res.* **2010**, *3*, 69.

[25] R. L. Penn, J. F. Banfield, *Science* **1998**, *281*, 969.
[26] a) O. Vidoni, K. Philippot, C. Amiens, B. Chaudret, O. Balmes, J. O. Malm, J. O. Bovin, F. Senocq, M. J. Casanove, *Angew. Chem.* **1999**, *111*, 3950; *Angew. Chem. Int. Ed.* **1999**, *38*, 3736; b) T. O. Ely, C. Amiens, B. Chaudret, *Chem. Mater.* **1999**, *11*, 526; c) K. Pelzer, O. Vidoni, K. Philippot, B. Chaudret, V. Collière, *Adv. Funct. Mater.* **2003**, *13*, 118.
[27] a) S. E. Habas, H. Lee, V. Radmilovic, G. A. Somorjai, P. Yang, *Nat. Mater.* **2007**, *6*, 692; b) F. R. Fan, D. Y. Liu, Y. F. Wu, S. Duan, Z. X. Xie, Z. Y. Jiang, Z. Q. Tian, *J. Am. Chem. Soc.* **2008**, *130*, 6949; c) B. Lim, J. Wang, P. H. C. Camargo, M. Jiang, M. J. Kim, Y. Xia, *Nano Lett.* **2008**, *8*, 2535; d) D. Seo, C. I. Yoo, J. Jung, H. Song, *J. Am. Chem. Soc.* **2008**, *130*, 2940; e) M. Tsuji, R. Matsuo, P. Jiang, N. Miyamae, D. Ueyama, M. Nishio, S. Hikino, H. Kumagae, K. S. N. Kamarudin, X. L. Tang, *Cryst. Growth Des.* **2008**, *8*, 2528; f) B. Lim, H. Kobayashi, T. Yu, J. Wang, M. J. Kim, Z.-Y. Li, M. Rycenga, Y. Xia, *J. Am. Chem. Soc.* **2010**, *132*, 2506.
[28] a) S. Zhou, K. McIlwrath, G. Jackson, B. Eichhorn, *J. Am. Chem. Soc.* **2006**, *128*, 1780; b) Z. Peng, H. Yang, *Nano Res.* **2009**, *2*, 406.
[29] B. Lim, M. Jiang, P. H. C. Camargo, E. C. Cho, J. Tao, X. Lu, Y. Zhu, Y. Xia, *Science* **2009**, *324*, 1302.
[30] Z. Peng, H. Yang, *J. Am. Chem. Soc.* **2009**, *131*, 7542.
[31] S. A. Bradford, *Corrosion Control*, 2nd ed., CASTI, Edmonton, **2001**, pp. 1–51.
[32] a) B. Wiley, T. Herricks, Y. Sun, Y. Xia, *Nano Lett.* **2004**, *4*, 1733; b) Y. Xiong, J. Chen, B. Wiley, Y. Xia, S. Aloni, Y. Yin, *J. Am. Chem. Soc.* **2005**, *127*, 7332; c) Y. Tang, M. Ouyang, *Nat. Mater.* **2007**, *6*, 754.
[33] Y. Xiong, B. Wiley, J. Chen, Z.-Y. Li, Y. Yin, Y. Xia, *Angew. Chem.* **2005**, *117*, 8127; *Angew. Chem. Int. Ed.* **2005**, *44*, 7913.
[34] C. M. Cobley, M. Rycenga, F. Zhou, Z.-Y. Li, Y. Xia, *J. Phys. Chem. C* **2009**, *113*, 16975.
[35] a) H. L. Nigg, L. P. Ford, R. I. Masel, *J. Vac. Sci. Technol. A* **1998**, *16*, 3064; b) H. L. Nigg, R. I. Masel, *J. Vac. Sci. Technol. A* **1998**, *16*, 2581.
[36] a) J. C. Hulteen, C. R. Martin, *J. Mater. Chem.* **1997**, *7*, 1075; b) C. R. Martin, *Acc. Chem. Res.* **1995**, *28*, 61.
[37] L. Carrette, K. A. Friedrich, U. Stimming, *Fuel Cells* **2001**, *1*, 5.
[38] a) N. M. Markovic, P. N. Ross, *Surf. Sci. Rep.* **2002**, *45*, 117; b) J. K. Nørskov, J. Rossmeisl, A. Logadottir, L. Lindqvist, J. R. Kitchin, T. Bligaard, H. Jónsson, *J. Phys. Chem. B* **2004**, *108*, 17886; c) H. A. Gasteiger, S. Kocha, B. Sompalli, F. T. Wagner, *Appl. Catal. B* **2005**, *56*, 9; d) V. R. Stamenkovic, B. Fowler, B. S. Mun, G. Wang, P. N. Ross, C. A. Lucas, N. M. Markovic, *Science* **2007**, *315*, 493.
[39] S. Guo, S. Dong, E. Wang, *ACS Nano* **2010**, *4*, 547.

